1-1-2014

Residual stresses in rail-ends from the in-service insulated rail joints using neutron diffraction

Vladimir Luzin
Australian Nuclear Science And Technology Organisation

Chandrahas Rathod
University of Wollongong, crr716@uowmail.edu.au

David Wexler
University of Wollongong, davidw@uow.edu.au

Paul Boyd
Central Queensland University

Manicka Dhanasekar
Queensland University of Technology

Residual stresses in rail-ends from the in-service insulated rail joints using neutron diffraction

Abstract

Insulated rail joints (IRJs) are an integral part of the rail track signaling system and pose significant maintenance and replacement costs due to their low and fluctuating service lives. Failure occurs mainly in rail head region, bolt-holes of fishplates and web-holes of the rails. Propagation of cracks is influenced by the evolution of internal residual stresses in rails during rail manufacturing (hot-rolling, roller-straightening, and head-hardening process), and during service, particularly in heavy rail haul freight systems where loads are high. In this investigation, rail head accumulated residual stresses were analysed using neutron diffraction at the Australian Nuclear Science and Technology Organisation (ANSTO). Two ex-service two head-hardened rail joints damaged under different loading were examined and results were compared with those obtained from an unused rail joint reference sample in order to differentiate the stresses developed during rail manufacturing and stresses accumulated during rail service. Neutron diffraction analyses were carried out on the samples in longitudinal, transverse and vertical directions, and on 5mm thick sliceed samples cut by Electric Discharge Machining (EDM). Ex-service rail samples, irrespective of loading conditions and service times, were found to have similar depth profiles of stress distribution. Evolution of residual stress fields in rails due to service was also accompanied by evidence of larger material flow. Stress evolution in the vicinity of rail ends was characterised by a compressive layer, approximately 5 mm deep, and a tension zone located approximately 5- 15mm below the surfaces. A significant variation of d0 with depth near the top surface was detected and was attributed to decarburisation in the top layer induced by cold work. Stress distributions observed in longitudinal slices of the two different deformed rail samples were found to be similar. For the undeformed rail, the stress distributions obtained could be attributed to variations associated with thermo-mechanical history of the rail.

Keywords

neutron, joints, insulated, service, diffraction, ends, residual, rail, stresses

Disciplines

Engineering | Science and Technology Studies

Publication Details

Luzin, V., Rathod, C., Wexler, D., Boyd, P. & Dhanasekar, M. (2014). Residual stresses in rail-ends from the in-service insulated rail joints using neutron diffraction. Materials Science Forum, 768-769 741-746.

Residual stresses in rail-ends from the in-service insulated rail joints using neutron diffraction

Vladimir Luzin[1, a], Chandrahas Rathod[2, b], David Wexler[2, c], Paul Boyd[3, d], Manicka Dhanasekar[4, e]

[1]Australian Nuclear Science & Technology Organisation, Lucas Heights, NSW, Australia

[2]Engineering faculty, Wollongong University, Northfields Ave, Wollongong, NSW, Australia

[3]Centre for Railway Engineering, Central Queensland University, Rockhampton, QLD, Australia

[4]Faculty of Built Environment & Engineering, QUT, Brisbane, QLD, Australia

[a]vll@ansto.gov.au, [b]crr716@uowmail.edu.au, [c]davidw@uow.edu.au, [d]p.boyd@cqu.edu.au, [e]m.dhanasekar@qut.edu.au,

Keywords: insulated rail joints, neutron diffraction, residual stress, accumulated stress, pearlitic steel, rail head.

Abstract

Insulated rail joints (IRJs) are an integral part of the rail track signaling system and pose significant maintenance and replacement costs due to their low and fluctuating service lives. Failure occurs mainly in rail head region, bolt- holes of fishplates and web-holes of the rails. Propagation of cracks is influenced by the evolution of internal residual stresses in rails during rail manufacturing (hot-rolling, roller-straightening, and head-hardening process), and during service, particularly in heavy rail haul freight systems where loads are high. In this investigation, rail head accumulated residual stresses were analysed using neutron diffraction at the Australian Nuclear Science and Technology Organisation (ANSTO). Two ex-service two head-hardened rail joints damaged under different loading were examined and results were compared with those obtained from an unused rail joint reference sample in order to differentiate the stresses developed during rail manufacturing and stresses accumulated during rail service.

Neutron diffraction analyses were carried out on the samples in longitudinal, transverse and vertical directions, and on 5mm thick sliceed samples cut by Electric Discharge Machining (EDM). Ex-service rail samples, irrespective of loading conditions and service times, were found to have similar depth profiles of stress distribution. Evolution of residual stress fields in rails due to service was also accompanied by evidence of larger material flow. Stress evolution in the vicinity of rail ends was characterised by a compressive layer, approximately 5 mm deep, and a tension zone located approximately 5- 15mm below the surfaces. A significant variation of d_0 with depth near the top surface was detected and was attributed to decarburisation in the top layer induced by cold work. Stress distributions observed in longitudinal slices of the two different deformed rail samples were found to be similar. For the undeformed rail, the stress distributions obtained could be attributed to variations associated with thermo-mechanical history of the rail.

Introduction

Insulated rail joint assemblies (Fig. 1) are primary components of rail track infrastructure and play a key role in track signaling systems and in the detection of rail fractures in track segments [1-3]. They generally comprise two rail ends separated by a narrow gap filled with insulator, and a fastening system including insulated side fishplates glued and bolted in place to improve rigidity [1]. IRJs have highly variable service lives with structural components failing under a range of modes, eventually resulting in overall failure of the joint. Metal flow is a key factor as the amount of surface rail deformation in the vicinity of rail ends is a generally greater than in continuous sections of rail. This can be attributed to a range of factors including; (i), that track sections comprising an IRJ are unbounded with a structural discontinuity across the rail joint and, (ii), that excessive interfacial friction is generated between the wheel and rail at the rail ends which experience a notch/damping effect. This effect imposes severe stress concentrations and causes plastic deformation and metal flow across the joints which can eventually leads to malfunction of the electrical insulation [2-4]. For all these reasons, significant efforts have been made to improve life-span of rail joints either by optimizing the structural design or by improving the mechanical properties of rail steel. As pearlitic rail steel has reached its upper damage tolerance limit, there has also been effort in finding alternative rail surfacing materials which can reduce track degradation in the vicinity of the insulating gap [4].

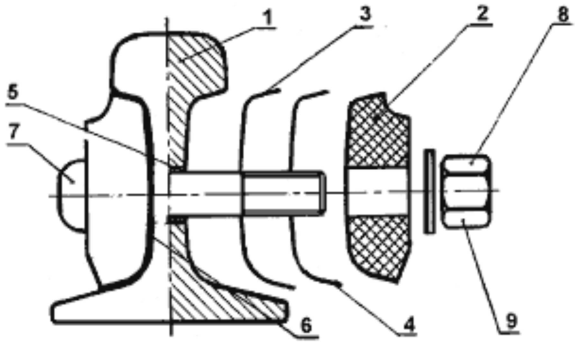

1. Rail, 2. Fishplate, 3. & 4. Insulators, 5. Bolt hole, 6. Insulator, 7. Bolt, 8. Nut, 9. Washer

Fig. 1. An Insulated Rail Joint assembly and its components.

As rail joints undergo plastic deformation during cyclic stress under rolling contact loading condition which results in a complex residual stress state near the surface and subsurface area of the rail head. Stresses are even more complex and intertwined near the rail joint due to its discontinuity in structure, and it is important to understand the stress development near the vicinity of rail joints and in subsurface region of the rail head. Stresses developed from a wheel/rail contact in service, exceeding the material yield point, can cause spalling fatigue cracking and can also produce head checking fatigue cracks.

Diffraction techniques are particularly suited to the non-destructive mapping of complex stress fields. Traditionally, neutron diffraction has been used to determine residual stresses internally in denser materials such as steel, where penetration depths are orders of magnitude greater than those of X-rays. Detailed 2-D and 3-D maps enable railway engineers to model and to better understand how residual stress fields are generated and to determine the most appropriate rail maintenance and replacement schedules for safe and economic operation. There are a handful of examples in the literature of use of neutron diffraction to investigate residual stresses in rail, including [5-8]. These investigations usually involve measurements of slices out of rails, like in the study on comparison of rails (slices) produced under different production conditions and investigations of residual stresses in wheel damaged track [8]. In this work, residual stresses in rail heads were analysed using the dedicated neutron residual stress diffractometer Kowari at the Australian Nuclear Science and Technology Organisation (ANSTO). In the current investigation, two IRJs with different rail service histories and accumulated damage were selected from the Queensland (Australia) heavy haul track service line. In addition, an unused IRJ fabricated from standard head hardened pearlitic steel track, was employed as a reference sample in order to differentiate the stresses developed during rail manufacturing and those developed during rail service.

Sample Preparation and Experimental

The end rail samples used for residual stress investigations comprised 400mm lengths of head hardened rail, obtained from disassembled 6-bolt square ended insulated rail joints. Three IRJs used are described as being in ‘as-manufactured‘, condition, ‘partly damaged‘ and ‘badly damaged‘, the latter having enough damage on inspection to require immediate removal from the Australian heavy haul rail track system. The 60 kg grade medium carbon rail steel is designated by Australian standard AS1085.12, with carbon content 0.65-0.82 wt.%

Measurements were made from intact rail ends in transverse (T) and longitudinal (L) directions at depths of 2, 4 and 6 mm from the top rail surfaces adjoining the rail ends. After that, 5mm thick slices were cut using electric discharge machining (EDM): transverse slices were cut from the middle part of the rail section while longitudinal slices were taken from ends of the rail section, as shown in Fig. 2. Residual stress measurements were carried out using the Kowari neutron residual stress scanner using 0.1672 nm neutron wavelength, Si(400) monochromator at $2\theta_M = 76^o$. In slices, the experiments were carried out using a gauge volume of 3×3×3 mm^3 and the Fe(211) reflection with the detector at the Bragg angle $2\theta_B$ of 90^o. The measuring time of 30 secs per point was typical to achieve accuracy of ~5x10^{-5} µstrains in strain scale and it was short enough to allow detailed stress mapping with large number of mesh points, 400 for L-slice and 355 for T-slices.

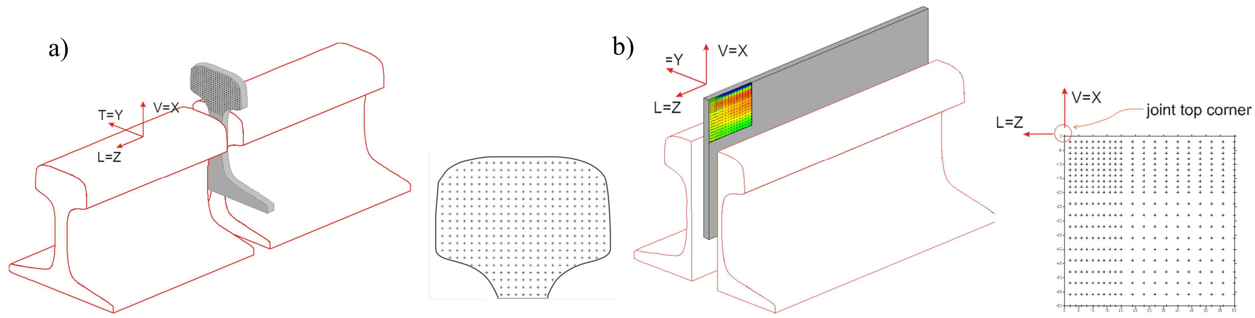

Fig. 2. Schematics of sample sections for neutron diffraction analysis, (a) T-slice and (b) L-slice.

Sectioned and polished samples were also examined unsig standard methods of reflected light microscopy, microhardness measurements (Leco Device) and secondary electron imaging (JEOL JSM 2001F instrument). Microhardness measurements were carried out along running surface of the rail head and across the gauge corner to access the extent of compressive stress shown in the transverse residual maps. A test load of 500g was selected, to measure the hardness distribution in the in-depth direction to about 20mm below the rail surface and at the gauge corner of the rail.

Results and Discussion

Microstructures of damaged rail samples Figure 3 shows representitative reflected light (Fig 3(a) - (b)) and SEM micrographs (Fig. 3(c)-(e)) of damaged rail samples. There was no evidence of white etching layer formation, but plastically deformed layers of depths ~25 µm and 60 µm below the running surface could be seen for the moderately deformed (Fig. 3(a)) and severely deformed (Fig. 3(b)) samples respectively. Below the deformed regions the bulk microstructures appeared free from any significant deformation.

Scanning electron microscopy (Fig. 3(c) – (e)) revealed deformormation of the cementite lamellae and reorientation towards the the direction of traffic movement. As indicated in Fig. 3(e), features including lamallae kinking, bending, globularisation and thinning in the rolling direction were evident in the deformed microstructure regions near the rail surfaces. Previous results [4] reveal that rail head spalling and sub-surface cracks are noticeable within few mm from the rail surface. As discussed in [9], crack originating subsurface regions tend to change direction, mostly either upward towards the rail surface or in some cases downwards. Because of this, the rail head material becomes detached from the surface resulting in spalling, causing failure of the rail.

Microhardness results Both deformed rail samples exhibited similar hardness profile trends from the top surface down in the T-sections (Fig. 4), while the unused rail sample exhibited little variation in hardness values across the measuring line. The maximum hardness value of 490HV were found near the running surface, while ~ 6 mm below the surface the hardness value changed to

~360HV, slightly higher than the bulk/unused rail hardness which falls in a range of 260-290HV. Hardness results obtained from longitudinal sections from the top down showed similar trands with a lower values further away form the rail ends.

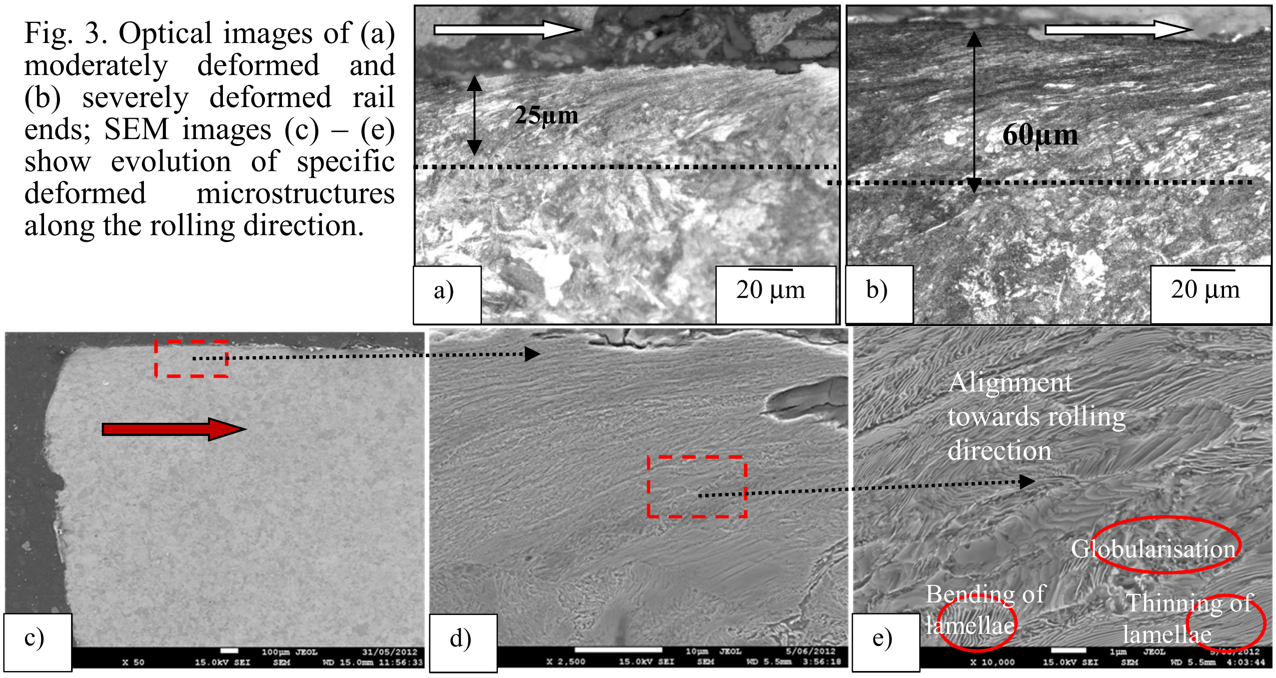

Fig. 3. Optical images of (a) moderately deformed and (b) severely deformed rail ends; SEM images (c) – (e) show evolution of specific deformed microstructures along the rolling direction.

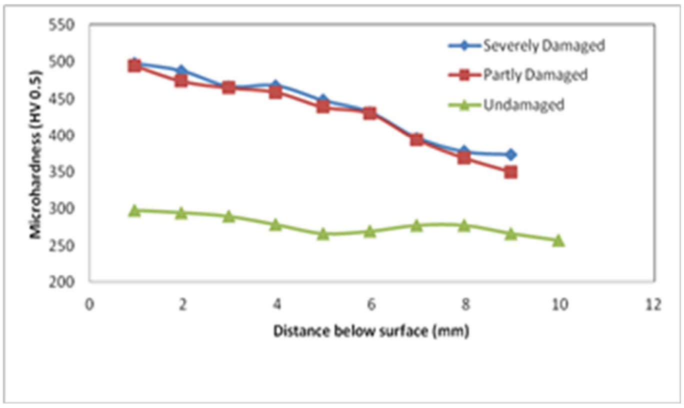

Fig. 4. Microhardness profiles as functions of depth below the suface near the rail end.

Residual stress maping.

Figure 5 shows the distribution of 2D residual stress maps in the slices from rail samples in different conditions. For both L and T slices, the stress distributions are dominated by compressive (~ -300 MPa) stresses (T component for the T-slices and L component for the L-slices) at the running surface and up to ~5 mm into the rail, which are balanced by tensile stresses (~ 200 MPa) located around 5-15 mm beneath. Both after-service rail samples exhibited similar stress distributions, although these were accentuated for the badly damaged rail.

While results for T-slices characterize stress distributions of continuous sections of rail (samples are taken away from the rail joint), results for L-slices demonstrate stress gradients in the proximity of the rail joint. To separate the effect of stress redistribution due to the presence of the rail end from the effect purely due to the different regime of material deformation in IRJ, diffirential stress maps, $\Delta\sigma_{xx}$ and $\Delta\sigma_{zz}$, were produced by subtracting stresses measured in the rail ends produced by EDM cutting (a byproduct of T-slice manufacturing) from stresses measured in the actual IRJ.

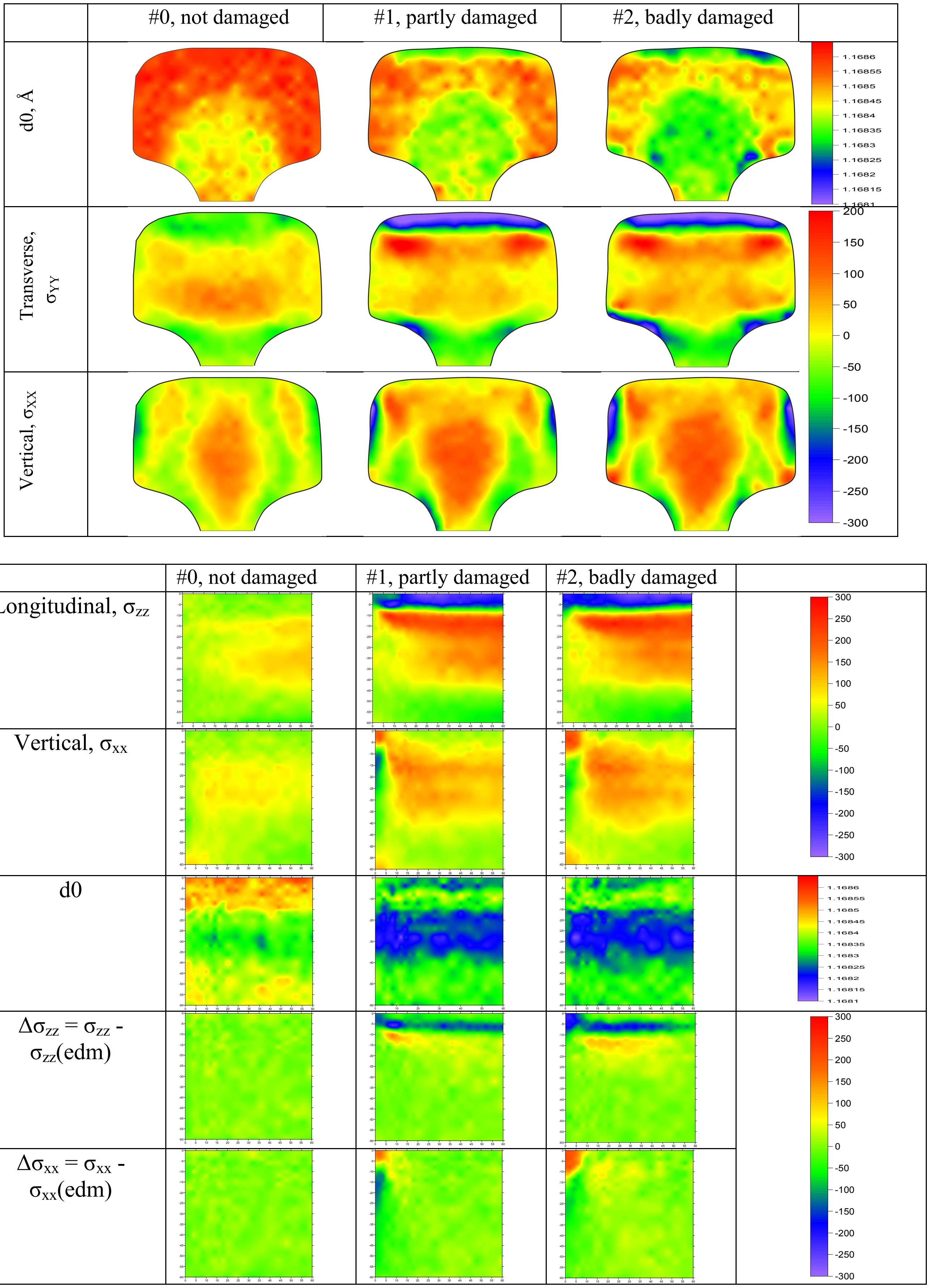

Fig. 5. 2D stress and d_0 maps for the T-slices (upper) and L-slices (lower). Compressive forces are blue, tensile forces are red. For the L slices both raw stress data and differential stress maps are shown. Square L-slice patch is 60 mm in size.

For the unused rail the 2D maps also revealed moderate tensile stresses in centre core of the rail head. These stresses are believed to be due to the roller straightening process during manufacturing. Compressive stresses are observed near the running surface and these are believed to have a beneficial role in resisting the further plastic deformation and growth of Rolling Contact fatigue (RCF) cracks. A significant variation of d_0 with depth near the top surface was detected and was attributed to decarburisation in the top layer induced by cold work.

Conclusions

Neutron diffraction of damaged IRJ samples revealed significant evolution of residual stress fields in rails due to service. Stress evolution in the bulk and vicinity of rail ends was characterised by a compressive layer, approximately 5-10 mm deep, and a tension zone located approximately 10-20 mm below the surfaces. A significant variation of d_0 with depth near the top surface was detected and was attributed to decarburisation in the top layer induced by cold work. Around the IRJ, material is more heavily deformed than material in the bulk of the rail as demonstrated from the longitudinal stress component differential maps $\Delta\sigma_{zz}$ in Fig.5: in the partially damaged rail the compression zone extends some 5 mm deeper than in the bulk areas, while for the badly damaged rail this effect even bigger and extend approximately 10 mm deeper than in a bulk part of the rail. Thus, although stress distributions observed in longitudinal slices of the two differently deformed rail samples seem to be similar, the badly damaged rail demonstrates deeper and stronger changes in the stress (and damage) state. This is also consistent with evidence of larger material flow based on light and scanning electron microscopy studies. For the undeformed rail, the stress distributions obtained could be attributed to variations associated with thermo-mechanical history of the rail.

Acknowledgements

This investigation forms a part of the Australian CRC for Rail Innovation research project, 'R3.100: longer life insulated rail joints' and was supported by an ANSTO in-kind grant for Beamtime proposal 1792. We also acknowledge the contribution of the Wollongong University Electron Microscopy Centre for provision of SEM services.

References

[1] Y. Hiroto: *Development of a long life Insulated Rail Joint*, Quarterly reports of the Railway Technical Research, Vol.25 (1984) p.79.
[2] C.Smalley: *Preliminary study into fatigue of Insulated Rail Joints*, Institute of Railway Technology at Monash University, (2009).
[3] J. Igwemezie, A.T. Nguyen: *Anatomy of joint bar failures II*, Railway Track & Structures, Vol. 105, Issue 10, (Oct 2009) p.43.
[4] C.Rathod, D.Wexler, T. Chandra, and H. Li, *Microstructural characterisation of railhead damage in insulated rail joints*, Materials Science Forum Vols. 706-709 (2012) p. 2937.
[5] T. Gnaupel-Herold, P.C. Brand, H.J. Prask, *Neutron Diffraction Investigation of Risidual Stresses in Transverse/Oblique Rail Slices Subjected to Different Grinding Stratagies*, Report NISTIR 6305, U.S. Department of Commerce, Technology Administration (1999).
[6] P.J. Webster, K.S. Low, G. Mills, and G.A. Webster, *Neutron Measurementsof Residual Stresses in a Used Raiway Rail*, Mat. Res. Soc Symp. Proc., 166, (1990) 311-316.
[7] G.A. Webster, P.J. Webster, M.A.M. Bourke, K.S. Low, G. Mills, H.J. McGillivray, D.F. Cannon and R.J. Allen, 1992, *Neutron Diffraction Determinations of Residual Stress Patterns in Railway Rails*, Mat. Res. Soc Symp. Proc 166, (1990) 143-152.
[8] V. Luzin, J.E. Gordon, T. Gnaupel-Herold and H.J. Prask, *Neutron residual stress measurements on rail sections for different production conditions*, Proc. IMECE04, 2004 ASME Int Mech Eng Congr. And Expn, Nov 13-20 (2004), Anaheim, CA, USA, 1-25.
[9] J. Tillberg, F.larson, K.Runesson, *A study of multiple crack interaction at rolling contact fatigue loading of rails,* Proc. I. Mech E Part F: J. Rail and Rapid Transit, 223 (2009) 319-330.